EUROPEAN ORGANIZATION FOR NUCLEAR RESEARCH

ANTIPROTON-PROTON ANNIHILATION INTO $\pi^+\pi^-$ AND K^+K^- AT 6.2 GeV/c

T. Buran[1)], Å. Eide[2,3)], P. Helgaker[1)], P. Lehmann[4)], A. Lundby, A. Navarro-Savoy[4)], L. Staurset[1)] and O. Sørum[1)]

CERN, Geneva, Switzerland

C. Baglin[5)], P. Fleury, G. de Rosny and J.M. Thenard[5)]

Ecole Polytechnique, Paris, France

P.J. Carlson[6)] and K.E. Johansson

University of Stockholm, Stockholm, Sweden

B. d'Almagne, F. Richard and D. Treille[6)]

Laboratoire de l'Accélérateur Linéaire, Orsay, France

V. Gracco

University of Genova and INFN, Genova, Italy

ABSTRACT

The angular distributions for the two annihilation channels $\bar{p}p \rightarrow \pi^+\pi^-$ and $\bar{p}p \rightarrow K^+K^-$ have been measured at 6.2 GeV/c. The two-pion channel, shows peripheral peaks for π^+ and π^- going forward, and the two-kaon channel shows a peripheral peak for the K^- going forward. The results have been compared with the line-reversed elastic backward scattering reactions and also with a constituent interchange model.

Geneva - 5 August 1976

(Submitted to Nuclear Physics B)

---

1) Present address: Department of Physics, University of Oslo, Norway.
2) Present address: Agder Regional College, Kristiansand, Norway.
3) Supported in part by Ecole Polytechnique, Paris, France.
4) Present address: CEA, Saclay, France.
5) Present address: LAPP, Annecy, France.
6) Now at CERN, Geneva, Switzerland.

1. INTRODUCTION

The study of the two diboson annihilation channels $\bar{p}p \to \pi^+\pi^-$ and $\bar{p}p \to K^+K^-$ can be divided into the low-energy region where direct channel effects dominate, and the high-energy region with peripheral peaks and a small differential cross-section around 90° c.m. The division between the two different regions we take to be somewhere around 3 GeV/c. The total cross-section for both channels decreases with energy following a power law in s, the total energy in the c.m. system squared, and attains for both channels a value close to 20 μb at an incident momentum of around 2.5 GeV/c.

In a recent experiment of Eisenhandler et al.[1] complete angular distributions have been measured for incident momenta from 0.8 to 2.4 GeV/c. Results from experiments using the bubble chamber technique have been reported for momenta up to 3.6 GeV/c [2-6].

In the high-energy region the peripheral peaks have been studied at 3 and 4 GeV/c by Brabson et al.[7] and at 6 and 8 GeV/c by Birnbaum et al.[8]. We have reported[9] earlier the measurement of a complete angular distribution at 5 GeV/c, within our experimental program.

The low-energy data have been analysed in terms of direct channel partial waves[10]. In the high-energy region the peripheral peaks have been interpreted in terms of baryon exchange and compared with elastic backward scattering using crossing[9,11]. The differential cross-section for a fixed, small t seems to decrease as s^{-3}. Recently much attention has been devoted to models for large-angle scattering, involving the interaction between point-like constituents of the elementary particles[12]. For the annihilation reactions, the differential cross-section at a fixed $\cos\theta_{cm}$ is predicted to drop as s^{-8}.

In this paper we report the results from a study of the annihilation reactions at an incident momentum of 6.2 GeV/c. Preliminary results were given at the London conference in 1974 [13]. We give here our final results and compare them with different models.

2. RESULTS AND DISCUSSIONS

The differential cross-sections, based on the number of accepted events, the acceptance calculation, and the correction factors[14], are given in Table 1 for the reaction $\bar{p}p \to \pi^-\pi^+$ and in Table 2 for $\bar{p}p \to K^-K^+$. For the annihilation into two pions a total of 326 good events was accumulated. Out of these, 254 were found in the forward hemisphere (characterized by the π^- going forward) and 72 were found in the backward hemisphere (the π^- going backward). For the annihilation into two kaons a total number of 162 good events were accumulated, all of them restricted to the forward hemisphere (the K^- going forward).

The errors are statistical only, based on the number of accepted events and on a smaller contribution from the acceptance calculation. The over-all normalization error is estimated at ±20%.

2.1 Experimental results

The differential cross-sections are shown in Figs. 1 and 2 together with corresponding data at 5 GeV/c [9]. The peripheral character of the annihilation reactions is clearly seen. For the reaction $\bar{p}p \to \pi^-\pi^+$, peaks for both the forward and backward directions are seen, while for the reaction $\bar{p}p \to K^-K^+$ only a peak in the forward direction is observed. The qualitative similarities between forward and backward scattering for $\bar{p}p \to \pi^-\pi^+$ and the striking differences between forward and backward scattering for $\bar{p}p \to K^-K^+$ -- features already observed in our previous experiment at 5 GeV/c [9] -- support the mechanism of baryon exchange. The difference between the forward and backward $\bar{p}p \to K^-K^+$ scattering stems from the lack of a baryon having strangeness +1, a consequence of which is the necessity of introducing, for example, a double exchange in order to describe the existence of the weak backward peak, observed at 5 GeV/c [9]. This also applies to K^-p backward elastic scattering. At 6.2 GeV/c the experiment was not sensitive enough to reveal the existence of a backward peak in this elastic channel[15].

2.2 Comparison with the line reversed reactions

We have compared $\bar{p}p \to \pi^-\pi^+$ with $\pi^\pm p$ elastic backward scattering and $\bar{p}p \to K^-K^+$ with K^+p elastic backward scattering. The annihilation reactions are connected with the elastic backward scattering ones via s-t crossing at fixed u. In order to compare matrix elements at given values of s, t (or u), spin and phase-space factors have to be taken into account. More specifically, we compare the differential cross-section for the annihilation reaction

$$\frac{d\sigma}{dt,u}\,(\bar{p}p \to M^-M^+) \tag{1}$$

with the corresponding elastic backward cross-section with the suitable spin and phase-space factors applied[11]:

$$\frac{(2s_M + 1)(2s_p + 1)}{(2s_{\bar{p}} + 1)(2s_p + 1)} \left(\frac{q_{Mp}}{q_{\bar{p}p}}\right)^2 \frac{d\sigma}{du}\,(M^\pm p \to pM^\pm)\ , \tag{2}$$

where M stands for π or K, s_M and s_p are the intrinsic spins, q_{Mp} and $q_{\bar{p}p}$ are the centre-of-mass momenta, evaluated at the same centre-of-mass energy.

This comparison is relevant only at the same c.m. energies and therefore the elastic backward cross-sections are scaled, using an s^{-2} dependence for πp and an s^{-3} dependence for Kp. The results of the comparisons are shown in Figs. 3-5.

The data are from Refs. 9, 15-17. In Fig. 3 the annihilation data for $\bar{p}p \rightarrow \pi^+\pi^-$, although of limited precision, agree with the data for $\pi^-p \rightarrow p\pi^-$ for $-t < 1.3\ (\mathrm{GeV}/c)^2$. For larger values of t no definite conclusions can be drawn.

When comparing $\bar{p}p \rightarrow \pi^-\pi^+$ with $\pi^+p \rightarrow p\pi^+$ (Fig. 4) there is an over-all agreement as far as the shapes of the cross-section distributions are concerned, but the magnitudes disagree by typically a factor of 2.

Finally, the annihilation data for $\bar{p}p \rightarrow K^-K^+$ are compared with data on $K^+p \rightarrow pK^+$ in Fig. 5. There is an over-all agreement.

The comparisons described above are of relevance only if the exchanged trajectories have the same signatures or if their amplitudes are orthogonal. The π^-p backward scattering is generally described as being due to Δ_δ exchange exclusively[11), and therefore the above-mentioned additional requirements for line reversal to hold, are not operative. The π^+p backward scattering is described as being due to the exchange of the N_α and Δ_δ trajectories, which have opposite signatures. The nucleon trajectory is, however, believed to dominate, inferring equality of Eqs. (1) and (2). The K^+p backward scattering is described in terms of the exchange of the Λ_α and Λ_γ trajectories, which are approximately exchange degenerate[18)].

From these considerations only, the equality of Eqs. (1) and (2) would be expected to be better obeyed by π^-p and K^+p elastic backward scattering than by π^+p. Our data support these considerations.

For the explanation of the apparent breaking of line reversal invariance, many factors can be invoked, such as contributions from other trajectories than those considered above, absorptive effects and direct channel effects, the last one losing effect with increasing energy.

2.3 Comparison with the parton interchange model

The parton interchange model proposed by Brodsky, Gunion and Blankenbecler[19)] predicts the differential cross-section to have a form given by

$$\frac{d\sigma}{dt} = \mathrm{const} \times s^{-N} \cdot f(\theta_{cm}) \ . \tag{3}$$

For the reaction $\bar{p}p \rightarrow \pi^-\pi^+$, N = 8 and, according to the model

$$f(\theta_{cm}) = \frac{1 - z^2}{2} \left[2(1 - z)^{-2} + (1 + z)^{-2}\right]^2 , \tag{4}$$

where $z = \cos\theta_{cm}$.

The constant is predicted to be the same as the one for $\pi^{\pm}p$ and $K^{\pm}p$ elastic scattering. For that reason we use the value of the constant determined for $\pi^{+}p$ elastic scattering at 10 GeV/c and at $\cos\theta_{cm} = 0$[20], which is 440 mb × GeV^{14}.

In Fig. 6 the experimental data at 5.0 (Ref. 9) and 6.2 GeV/c are shown together with the predictions by the parton interchange model (Ref. 19), the latter indicated with a broken line and a full line, respectively. Mainly in the backward direction (the π^- going backward) a good agreement can be seen. At 6.2 GeV/c the agreement is rather good in both the forward and the backward regions. In the region around $\cos\theta_{cm} = 0$, where the model is believed to be more appropriate, no data at 6.2 GeV/c exist. At 5.0 GeV/c the predicted values are 1.5 standard deviations below the ones experimentally determined.

2.4 Energy dependence at small |t|

The energy dependence of the differential cross-section at small, fixed momentum transfer gives information on the underlying exchange mechanism. We have noted earlier[9] that for incident momenta smaller than 2-3 GeV/c, the differential cross-section for a fixed small momentum transfer decreases rapidly with s (like s^{-10}). For momenta exceeding 2-3 GeV/c this energy dependence is drastically different for the annihilation channels for which baryon exchange is an allowed mechanism. This is interpreted as being due to the domination of the baryon exchange mechanism, giving an energy dependence characteristic of the exchanged baryon trajectory, like s^{-2} for annihilation into pions and s^{-3} for annihilation into kaons.

In Fig. 7 we show the angular distribution for the annihilation into $\pi^-\pi^+$ obtained in this experiment for the region $|t| < 1.5$ $(GeV/c)^2$. Our data extend down to $-t = 0.4$ $(GeV/c)^2$. Also, we show a lower $|t|$ point at 6 GeV/c (Ref. 8). The curves represent the predictions from line reversal (Section 2.2), using data on π^+p elastic backward scattering at 5 and 7 GeV, respectively. The figure illustrates the difficulty in assigning a value to the differential cross-section for a $|t|$ value of 0.3 to 0.4 $(GeV/c)^2$. We have therefore made no further study of the energy dependence for the $\pi^+\pi^-$ channel.

In Fig. 8 we show the energy variation of $d\sigma/dt$ at $-t = 0.3$ $(GeV/c)^2$ for the channel $\bar{p}p \rightarrow K^-K^+$. Data are from Refs. 1, 4, 7, and 9. Fits to the form $d\sigma/dt = \text{const} \times s^{-\alpha}$ give $\alpha = 3.6 \pm 0.2$ and $\alpha = 8.5 \pm 0.6$ for the two cases K^- forward and K^+ forward, respectively. These results agree with the corresponding elastic backward scattering data, giving $\alpha = 4.3 \pm 0.3$ for K^+p (Ref. 20) and $\alpha = 9.8 \pm 0.4$ for K^-p (Ref. 9). The sketched dotted curve is a prediction from line reversal (Section 2.2) using the fit to K^+p elastic backward scattering data[20]. We conclude from this figure that the line reversal prediction agrees with the data above an incident momentum of 2-3 GeV/c. The data displayed in Fig. 8 do not show the change of slope as observed earlier[9].

3. SUMMARY

The study of the two annihilation channels $\bar{p}p \rightarrow \pi^+\pi^-$ and $\bar{p}p = K^+K^-$ at 6.2 GeV/c incident momentum has revealed that

i) there is a rapid energy variation of the differential cross-section at a fixed t or cos θ_{cm} between 5 and 6.2 GeV/c;

ii) there is a fair agreement between the data for the annihilation reactions and the corresponding line-reversed elastic backward scattering reactions;

iii) the angular distribution at 6.2 GeV/c for the annihilation into pions agrees quite well with a parton model;

iv) for the two-kaon channel no events have been observed with the K^+ going forward, in agreement with baryon exchange as the underlying mechanism. No baryon with the quantum numbers required to be exchanged in this channel is known.

REFERENCES

1) E. Eisenhandler, W.R. Gibson, C. Hojvat, P.I.P. Kalmus, L.C.Y. Lee, T.W. Pritchard, E.C. Usher, D.T. Williams, M.A. Harrison, W.H. Range, M.A.R. Kemp, A.D. Rush, J.N. Woulds, G.T.J. Arnison, A. Astbury, D.P. Jones and A.S.L. Parsons, Nuclear Phys. B96, 109 (1975).

2) M.A. Mandelkern, R.R. Burns, P.E. Condon and J. Schultz, Phys. Rev. D 4, 2658 (1971).

3) T. Bacon, I. Butterworth, R.J. Miller, J.J. Phelan, R.A. Donald, D.N. Edwards, D. Howard and R.S. Moore, Phys. Rev. D 7, 577 (1973).

4) T. Fields, W.A. Cooper, D.S. Rhines, J. Whitmore and W.W.M. Allison, Phys. Letters 40B, 503 (1972).

5) V. Domingo, G.P. Fisher, L. Marshall Libby and R. Sears, Phys. Letters 24B, 642 (1967).

6) W.M. Katz, B. Forman and F. Ferbel, Phys. Rev. Letters 19, 265 (1967).

7) A. Brabson, G. Calvelli, S. Cittolin, P. De Guio, F. Gasparini, S. Limentani, P. Mittner, M. Posocco, L. Ventura, C. Voci, M. Crozon, A. Diaczek, R. Sidwell and J. Tocqueville, Phys. Letters 42B, 287 (1972).

8) D. Birnbaum, R.M. Edelstein, N.C. Hien, T.J. McMahon, J.F. Mucci, J.S. Russ, E.W. Anderson, E.J. Bleser, H.R. Blieden, G.B. Collins, D. Garelick, J. Menes and F. Turkot, Phys. Rev. Letters 23, 433 (1969).

9) Å. Eide, P. Lehmann, A. Lundby, C. Baglin, P. Briandet, P. Fleury, P.J. Carlson, E. Johansson, M. Davier, V. Gracco, R. Morand and D. Treille, Nuclear Phys. B60, 173 (1973).

10) See, for example, A. Donnachie and P.R. Thomas, Nuovo Cimento 26A, 317 (1975).

11) J.D. Jackson, Duality and exchange degeneracy in high-energy phenomenology, *in* Proc. Internat. Conf. on Duality and Symmetry in Hadron Physics, Tel Aviv, 1971 (ed. E. Gotsman)(Weizmann Science Press of Israel, Jerusalem, 1971), p. 1.
A. Białas and O. Czyzewski, Phys. Letters 13, 337 (1964).
V. Barger and D. Cline, Phys. Letters 25, 415 (1967).

12) D. Sivers, S.J. Brodsky and R. Blankenbecler, Physics Reports 23C, 1 (1976).

13) T. Buran, Å. Eide, P. Helgaker, P. Lehmann, A. Lundby, A. Navarro-Savoy, L. Staurset, O. Sörum, C. Baglin, P. Briandet, P. Fleury, G. de Rosny, J.M. Thenard, P.J. Carlson, K.E. Johansson, B. d'Almagne, F. Richard, D. Treille and V. Gracco, K^-p and $\bar{p}p$ elastic scattering and two-body annihilations at 6.2 GeV/c, Submitted to the 17th Internat. Conf. on High-Energy Physics, London, 1974.

14) T. Buran, Å. Eide, P. Helgaker, P. Lehmann, A. Lundby, A. Navarro-Savoy, L. Staurset, O. Sörum, C. Baglin, P. Briandet, P. Fleury, G. de Rosny, J.M. Thenard, P.J. Carlson, K.E. Johansson, B. d'Almagne, F. Richard, D. Treille and V. Gracco, Nuclear Phys. B97, 11 (1975).

15) T. Buran, Å. Eide, P. Helgaker, P. Lehmann, A. Lundby, A. Navarro-Savoy, L. Staurset, O. Sörum, C. Baglin, P. Briandet, P. Fleury, G. de Rosny, J.M. Thenard, P.J. Carlson, K.E. Johansson, B. d'Almagne, F. Richard, D. Treille and V. Gracco, π^-p and K^-p elastic scattering at 6.2 GeV/c, Submitted to Nuclear Physics B.

16) D.P. Owen, F.C. Peterson, J. Orear, A.L. Read, D.G. Ryan, D.H. White, A. Ashmore, C.J.S. Damerell, W.R. Frisken and R. Rubinstein, Phys. Rev. 181, 1794 (1969).

17) W.F. Baker, K. Berkelman, P.J. Carlson, G.P. Fisher, P. Fleury, D. Hartill, K. Kalbach, A. Lundby, S. Mukhin, R. Nierhaus, K.P. Pretzl and J. Woulds, Nuclear Phys. B25, 385 (1971).

18) J. Banaigs, J. Berger, C. Bonnel, J. Duflo, L. Goldzahl, F. Plouin, W.F. Baker, P.J. Carlson, V. Chabaud and A. Lundby, Nuclear Phys. B9, 640 (1969).

19) J.F. Gunion, S.J. Brodsky and R. Blankenbecler, Phys. Rev. D 8, 287 (1973).

20) C. Baglin, P. Briandet, P. Fleury, G. de Rosny, P.J. Carlson, K.E. Johansson, B. d'Almagne, P. Lehmann, M. Richard, D. Treille, Å. Eide, A. Lundby, A. Navarro-Savoy, L. Staurset and V. Gracco, Nuclear Phys. B98, 365 (1975).

Table 1

Differential cross-sections for $\bar{p}p \rightarrow \pi^-\pi^+$ at 6.21 GeV/c. The quoted errors are statistical. Systematic errors are estimated at ±20%. $s = 13.546$ GeV^2, $t + u = -11.746$ (GeV/c)^2. Kinematic limits: $-t = 0.063$ and $-t = 11.683$ (GeV/c)^2.

$-t$ [(GeV/c)^2]	Δt [(GeV/c)^2]	$\cos\theta_{cm}$	$d\sigma/dt$ [nb/(GeV/c)^2]	Error [nb/(GeV/c)^2]
0.45	0.1	0.933	670	130
0.55	0.1	0.916	650	130
0.65	0.1	0.899	940	160
0.75	0.1	0.882	830	150
0.85	0.1	0.865	700	140
0.95	0.1	0.847	590	130
1.05	0.1	0.830	600	140
1.15	0.1	0.813	520	140
1.30	0.2	0.787	274	70
1.50	0.2	0.753	172	55
1.70	0.2	0.718	149	55
1.90	0.2	0.683	141	55
2.10	0.2	0.649	157	63
2.30	0.2	0.615	64	45
2.70	0.6	0.546	38	22
9.10	0.8	-0.555	16	12
9.75	0.5	-0.667	20	14
10.25	0.5	-0.753	48	20
10.60	0.2	-0.814	97	40
10.80	0.2	-0.848	117	47
11.00	0.2	-0.882	94	39
11.20	0.2	-0.917	180	47
11.45	0.3	-0.960	180	39

Table 2

Differential cross-sections for $\bar{p}p \to K^-K^+$ at 6.21 GeV/c. The quoted errors are statistical. Systematic errors are estimated at ±20%. $s = 13.546$ GeV^2. Kinematic limits: $-t = 0.036$ and $-t = 11.262$ (GeV/c)^2.

$-t$ [(GeV/c)^2]	Δt [(GeV/c)^2]	$\cos\theta_{cm}$	$d\sigma/dt$ [nb/(GeV/c)^2]	Error [nb/(GeV/c)^2]
0.35	0.1	0.944	940	230
0.45	0.1	0.926	920	170
0.55	0.1	0.908	1060	200
0.65	0.1	0.891	274	94
0.75	0.1	0.873	490	130
0.85	0.1	0.855	630	150
0.95	0.1	0.837	310	110
1.05	0.1	0.819	460	130
1.20	0.2	0.793	134	51
1.40	0.2	0.757	110	45
1.75	0.5	0.695	28	16
2.25	0.5	0.606	26	18
3.00	1.0	0.472	15	upper limit

Figure captions

Fig. 1 : The angular distributions for the channel $\bar{p}p \to \pi^-\pi^+$ measured at 6.2 GeV/c (this experiment) and at 5 GeV/c (Eide et al., Ref. 9).

Fig. 2 : The angular distribution in the forward direction for the channel $\bar{p}p \to K^-K^+$. Data at 6.2 GeV/c are from this experiment, at 5 GeV/c from Eide et al. (Ref. 9).

Fig. 3 : Differential cross-sections for $\bar{p}p \to \pi^+\pi^-$ (π^+ forward) at 6.2 GeV/c compared with data on π^-p backward elastic scattering from Owen et al. at 5.9 GeV/c (Ref. 16), Buran et al. at 6.2 GeV/c (Ref. 15), and from Baker et al. at 7.0 GeV/c (Ref. 17). The π^-p data have first been scaled to $s = 13.53$ GeV^2 ($\bar{p}p$ at 6.2 GeV/c and πp at 6.73 GeV/c) according to $d\sigma/du = \text{const} \times s^{-2}$, then multiplied with the crossing factor 0.589 (see text).

Fig. 4 : Differential cross-sections for $\bar{p}p \to \pi^-\pi^+$ (π^- forward) at 6.2 GeV/c compared with data on π^+p backward elastic scattering from Eide et al. (Ref. 9) at 5.0 GeV/c and from Baker et al. (Ref. 17) at 7.0 GeV/c. The π^+p data have first been scaled to $s = 13.53$ GeV^2 ($\bar{p}p$ at 6.2 GeV/c and πp at 6.73 GeV/c) according to $d\sigma/du = \text{const} \times s^{-2}$, then multiplied with the crossing factor 0.589 (see text).

Fig. 5 : Differential cross-sections for $\bar{p}p \to K^-K^+$ (K^- forward) at 6.2 GeV/c compared with the K^+p backward elastic scattering data of Eide et al. (Ref. 9) at 5.0 GeV/c. The latter have first been scaled to $s = 13.53$ GeV^2 ($\bar{p}p$ at 6.2 GeV/c and Kp at 6.60 GeV/c) according to $d\sigma/du = \text{const} \times s^{-3}$, then multiplied with the crossing factor 0.567 (see text).

Fig. 6 : The angular distribution for the channel $\bar{p}p \to \pi^-\pi^+$ as a function of $\cos\theta_{cm}$. Data from this experiment at 6.2 GeV/c and from Eide et al. (Ref. 9) at 5 GeV/c. The full and the broken lines are the predictions from the constituent interchange model for 6.2 and 5 GeV/c, respectively.

Fig. 7 : Differential cross-section for the channel $\bar{p}p \to \pi^-\pi^+$ (π^- going forward) as a function of $-t$. Data from this experiment at 6.2 GeV/c and from Birnbaum et al. (Ref. 8). The broken curves are predictions from line reversal using data on π^+p backward elastic scattering (see Section 2.2 and Fig. 4).

Fig. 8 : Differential cross-sections at $-t = 0.3$ (GeV/c)^2 for the annihilation reaction $\bar{p}p \to K^-K^+$ as a function of s. Data from Eisenhandler et al. (Ref. 1) (12 points between 0.79 and 2.43 GeV/c incident momentum), from Fields et al. (Ref. 4) at 2.3 GeV/c, from Brabson et al. (Ref. 5)

at 3 and 4 GeV/c, from Eide et al. (Ref. 9) at 5 GeV/c and from this experiment at 6.2 GeV/c. The broken line is a prediction from line reversal using the fit to K^+p backward elastic scattering of Baglin et al. (Ref. 20). The backward differential cross-section for $-u = 0.3$ $(GeV/c)^2$ at a given s-value has been multiplied by the crossing factor $\frac{1}{2}\, q^2(Kp)/q^2(\bar{p}p)$, where $q(Kp)$ and $q(\bar{p}p)$ are the c.m. momenta for Kp and the $\bar{p}p$ system respectively (see Section 2.2). The straight lines are least squares fits to the data (see text).

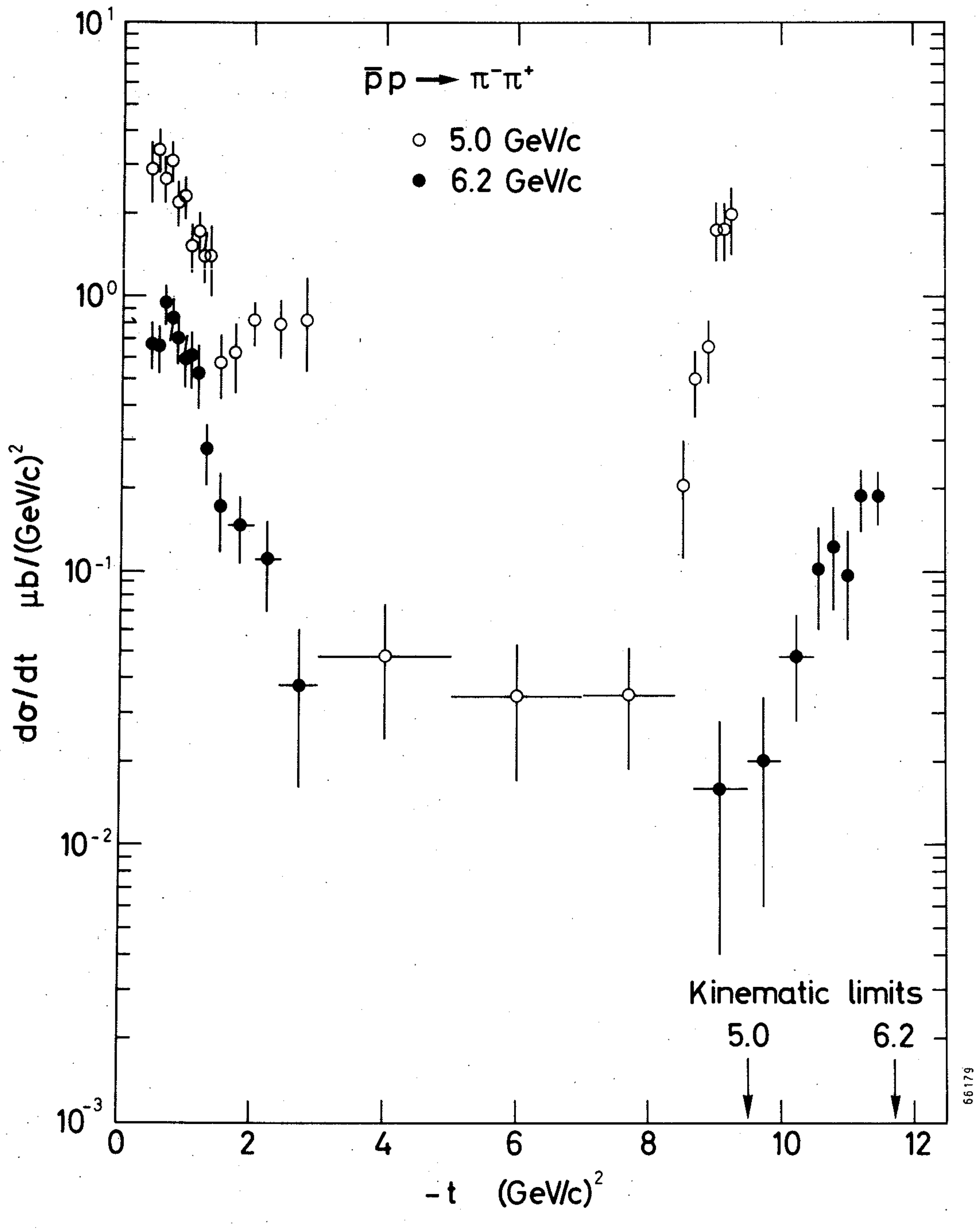
$\bar{p}p \rightarrow \pi^-\pi^+$
5.0 GeV/c
6.2 GeV/c
10^1
10^0
10^{-1}
10^{-2}
10^{-3}
dσ/dt μb/(GeV/c)^2
0
2
4
6
8
10
12
-t (GeV/c)^2
Kinematic limits
5.0
6.2
66179

Fig. 1

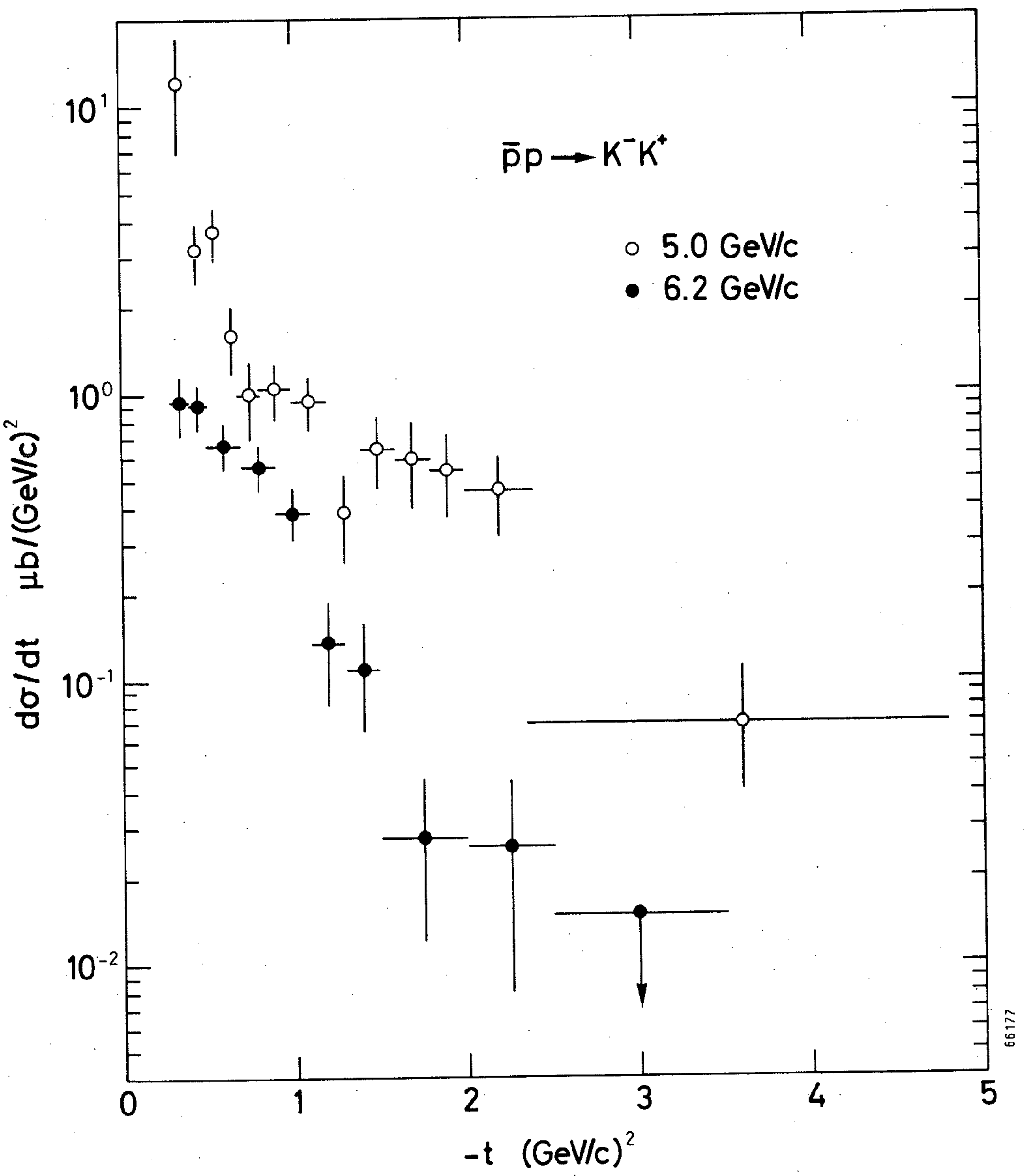

$\bar{p}p \to K^-K^+$
○ 5.0 GeV/c
● 6.2 GeV/c
$d\sigma/dt \quad \mu b/(GeV/c)^2$
$-t \quad (GeV/c)^2$
10^1
10^0
10^{-1}
10^{-2}
0
1
2
3
4
5
66177

Fig. 2

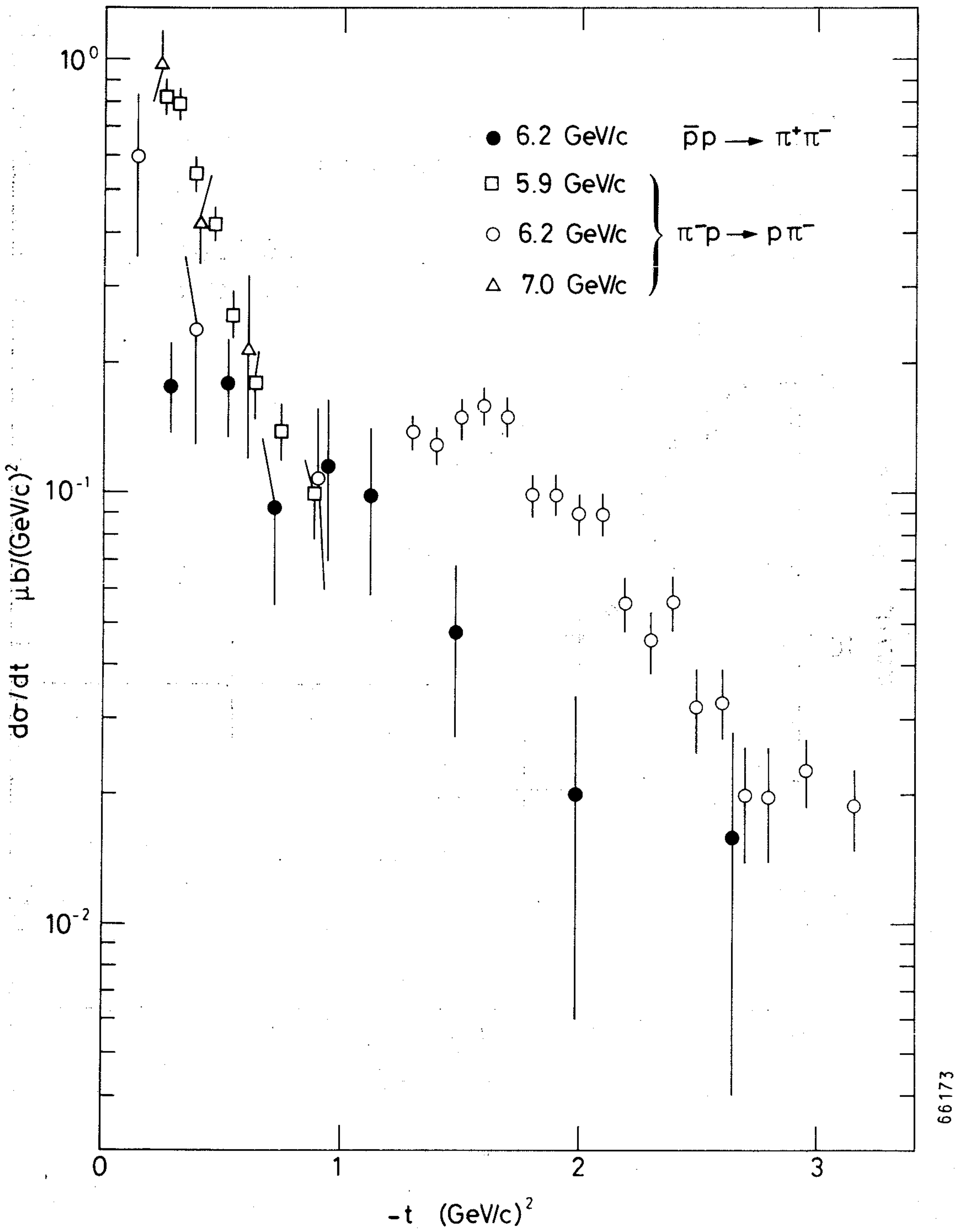

6.2 GeV/c
$\bar{p}p \to \pi^+\pi^-$
5.9 GeV/c
6.2 GeV/c
$\pi^-p \to p\pi^-$
7.0 GeV/c
10^0
10^{-1}
10^{-2}
$d\sigma/dt \quad \mu b/(GeV/c)^2$
0
1
2
3
$-t \quad (GeV/c)^2$
66173

Fig. 3

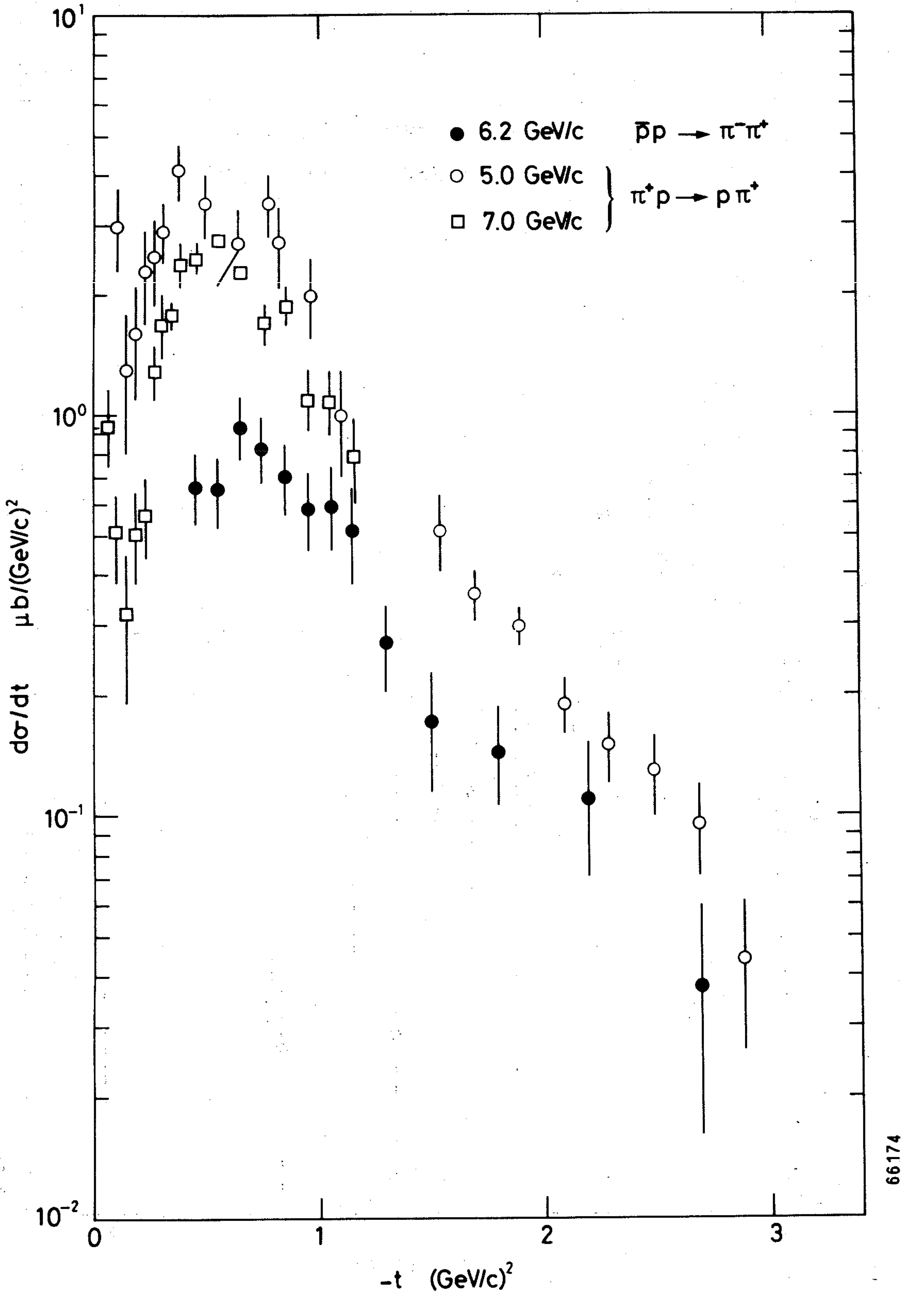

10¹
10⁰
10⁻¹
10⁻²
dσ/dt μb/(GeV/c)²
● 6.2 GeV/c p̄p → π⁻π⁺
○ 5.0 GeV/c
□ 7.0 GeV/c
π⁺p → pπ⁺
0
1
2
3
-t (GeV/c)²
66174

Fig. 4

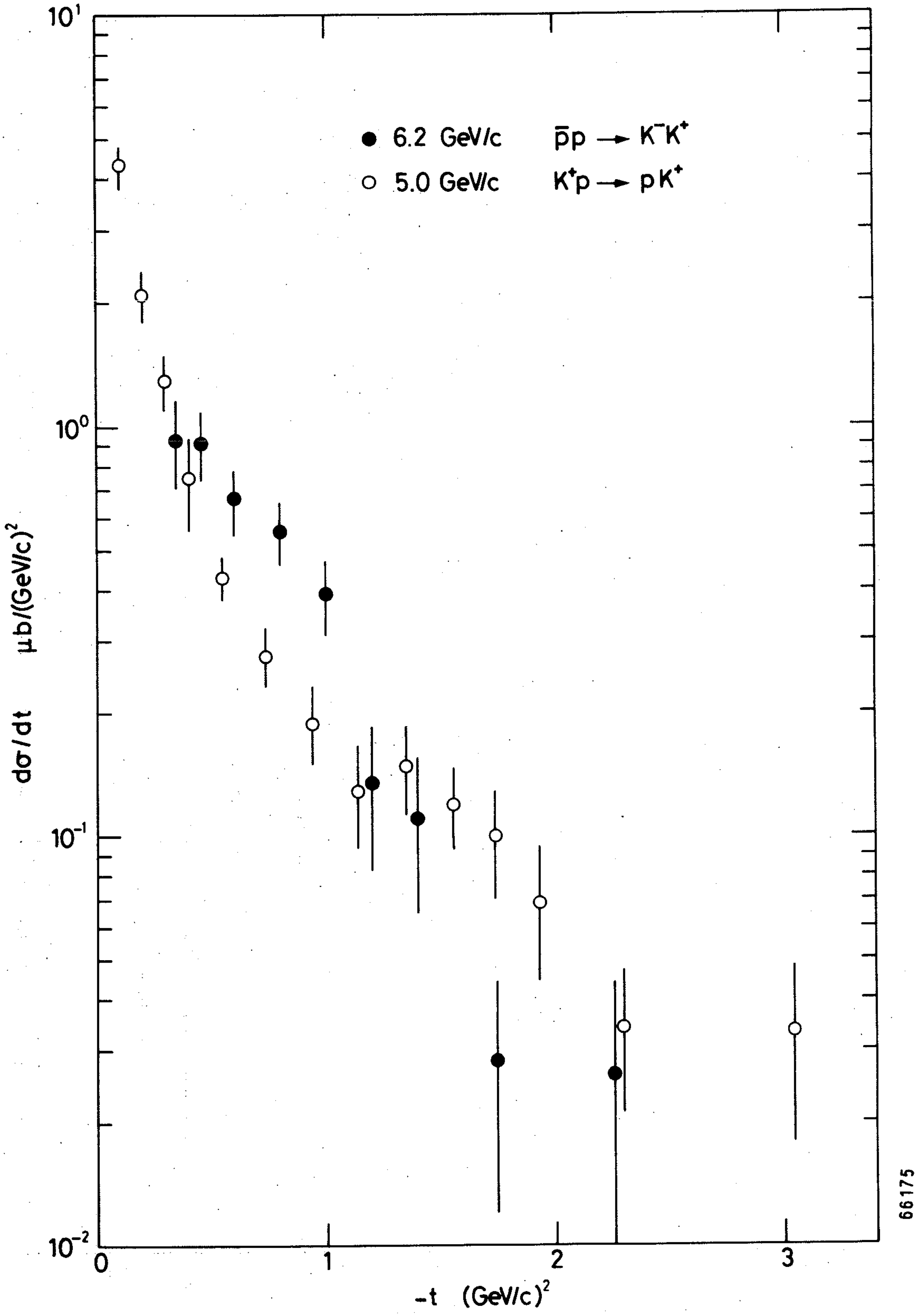
6.2 GeV/c $\bar{p}p \rightarrow K^-K^+$
5.0 GeV/c $K^+p \rightarrow pK^+$
10^1
10^0
10^{-1}
10^{-2}
$d\sigma/dt$ $\mu b/(GeV/c)^2$
0
1
2
3
$-t$ $(GeV/c)^2$
66175

Fig. 5

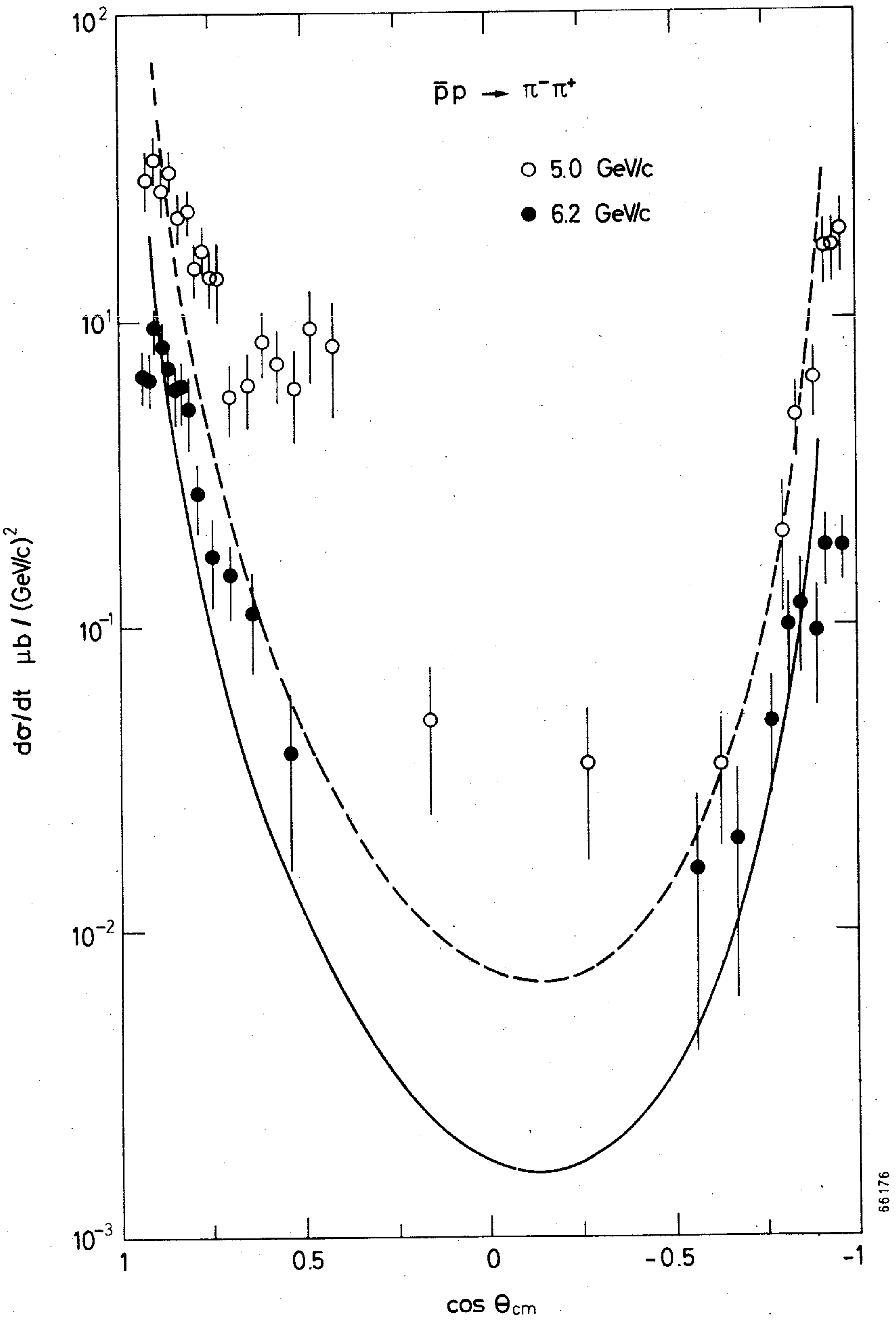

p̄p → π⁻π⁺
○ 5.0 GeV/c
● 6.2 GeV/c
dσ/dt μb / (GeV/c)²
10²
10¹
10⁻¹
10⁻²
10⁻³
1
0.5
0
-0.5
-1
cos θcm
66176

Fig. 6

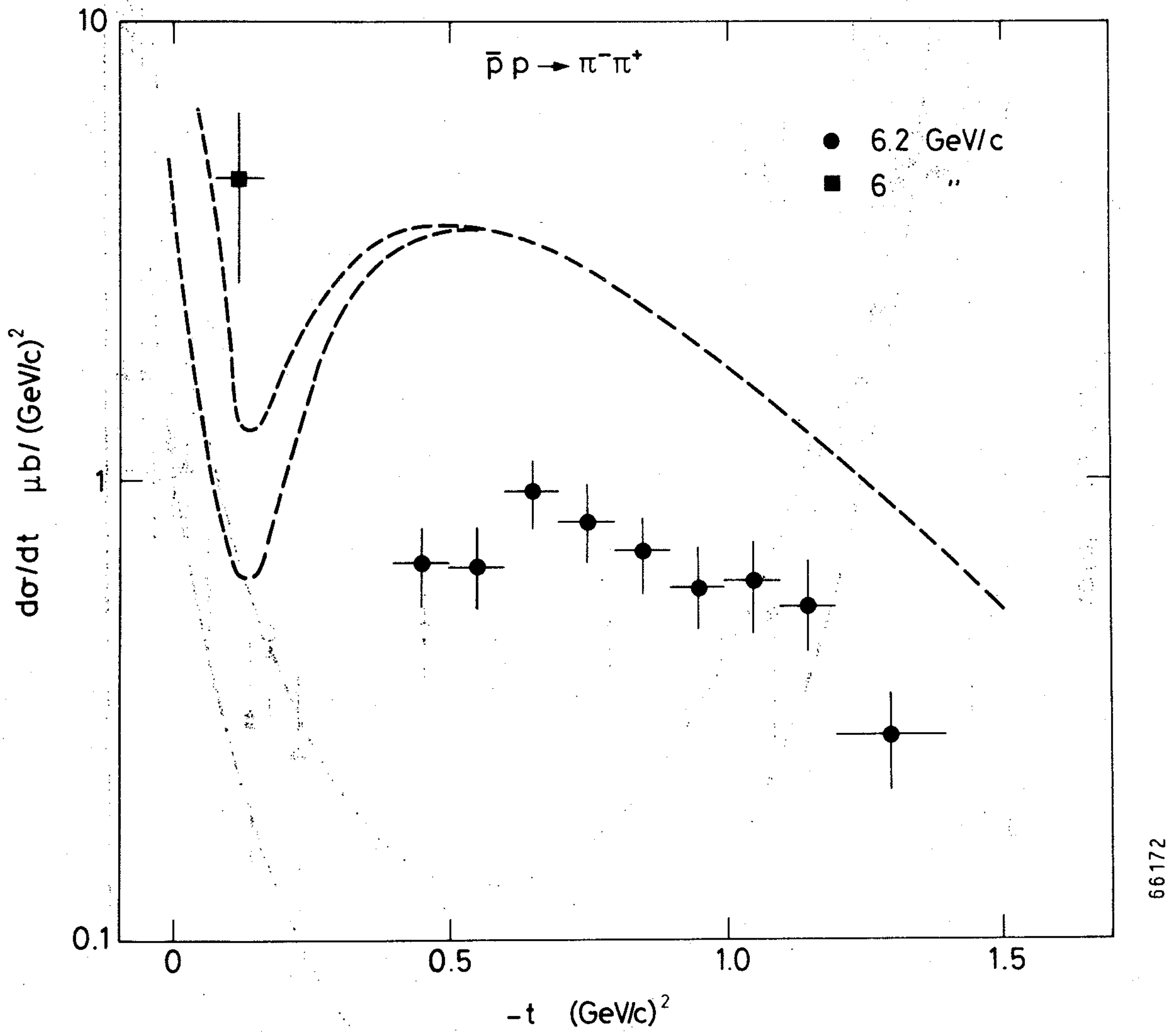

$\bar{p}p \rightarrow \pi^-\pi^+$
6.2 GeV/c
6 "
10
1
0.1
$d\sigma/dt \quad \mu b/(GeV/c)^2$
0
0.5
1.0
1.5
$-t \quad (GeV/c)^2$
66172

Fig. 7

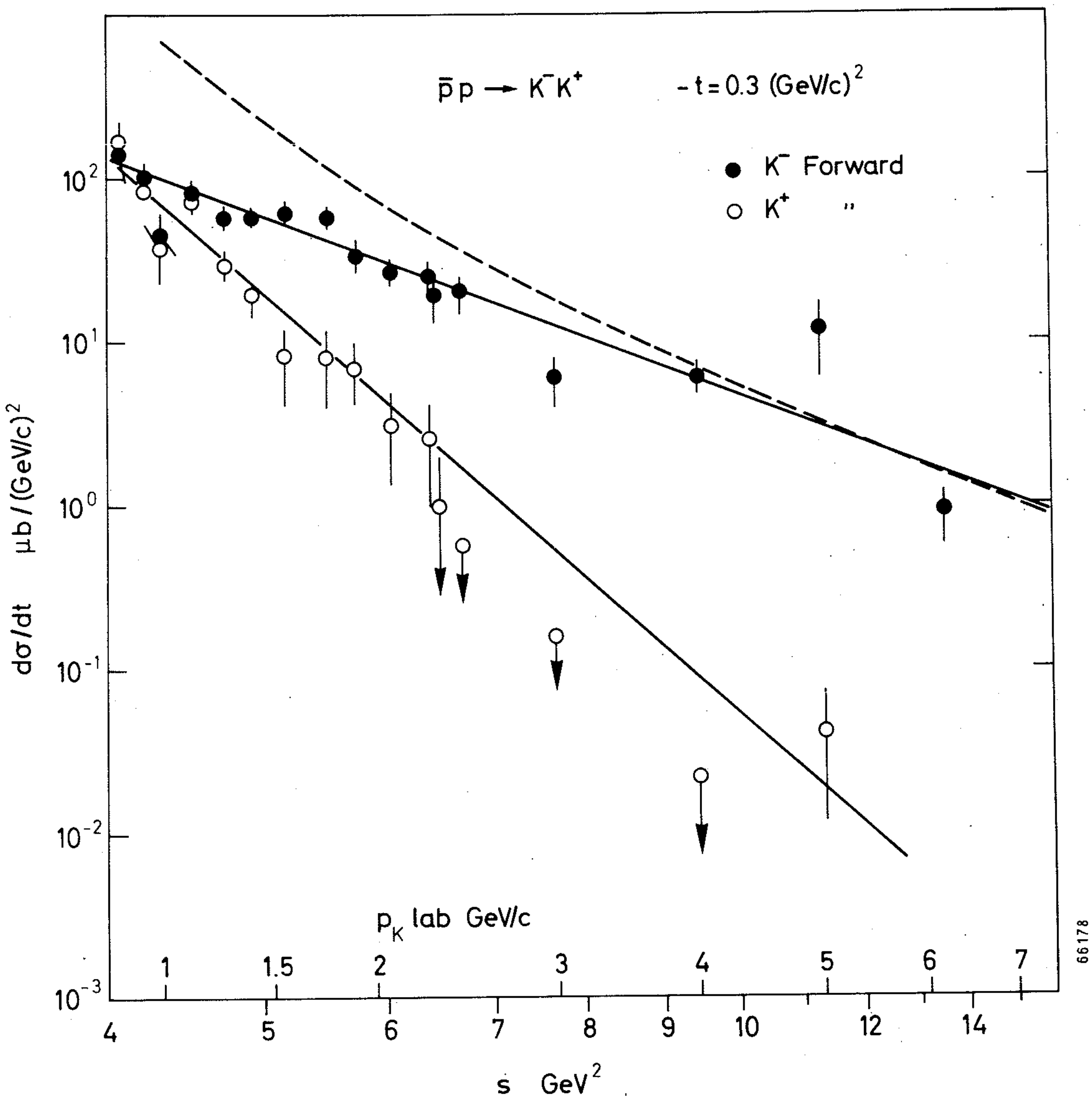

p̄p → K⁻K⁺ -t = 0.3 (GeV/c)²
K⁻ Forward
K⁺ "
dσ/dt μb/(GeV/c)²
10²
10¹
10⁰
10⁻¹
10⁻²
10⁻³
p_K lab GeV/c
1
1.5
2
3
4
5
6
7
4
5
6
7
8
9
10
12
14
s GeV²
66178

Fig. 8